Polymer Chemistry

PAPER

A furan-bridged D-π-A copolymer with deep HOMO level: synthesis and application in polymer solar cells

Xiaochen Wang,[a] Song Chen,[ac] Yeping Sun,[ab] Maojie Zhang,[b] Yongfang Li,*[b] Xiaoyu Li*[a] and Haiqiao Wang*[a]

A novel D-π-A copolymer, **PFBT-BDT**, based on furan-containing benzothiadiazole (**FBT**) and benzodithiophene (**BDT**) was designed and synthesized by Pd-catalyzed Stille-coupling method. The copolymer showed good solubility and film-forming ability combining with good thermal stability. **PFBT-BDT** exhibited a broad absorption from 300 to 630 nm with an absorption peak centered at 522 nm. The optical band gap (E_g^{opt}) determined from the onset of absorption of the polymer film was 1.96 eV. The LUMO and HOMO energy levels of the polymer were estimated to be −3.48 eV and −5.44 eV, respectively. The polymer solar cell fabricated from the blend of the polymer as donor and PC$_{71}$BM as acceptor exhibited a moderate power conversion efficiency of 2.81% with a high V_{oc} of 0.94 V without annealing and any additives. To the best of our knowledge, this is among the highest V_{oc} values for PSCs based on benzodithiophene derivatives. This work demonstrates that the replacement of thiophene moieties in conjugated polymers with more electron-withdrawing furan moieties is able to significantly lower the HOMO energy levels, and therefore, increase the open circuit voltage of solar cells.

Introduction

Bulk heterojunction (BHJ) polymer solar cells (PSCs) have attracted tremendous interest due to their potential applications in large area, light weight, flexible photovoltaic devices through low-cost solution-processable techniques. In recent years, great efforts have been made to improve the power conversion efficiency (PCE) of the PSCs by designing and synthesizing new conjugated polymer materials.[1–9] But nearly all high-performance devices reported so far rely on thiophene-based conjugated polymers. There is only a small amount of research focus on nonthiophene heterocycles-based conjugated polymer materials. Recently, Walker *et al.*[10] reported a benzofuran-substituted diketopyrrolopyrrole derivative which has one of the best performances among organic solar cells based on small molecules. More recently, Woo *et al.*[11] used furan as an alternative to thiophene in conjugated polymers for application in PSCs. They found that furan-containing polymers exhibited similar optical and electronic properties relative to their thiophene counterparts. As a result, PSCs fabricated from furan-containing polymers and

PC$_{71}$BM as the acceptor showed power conversion efficiencies reaching 5%, which indicating the potential of furans as thiophene alternatives in the design of high-performance organic solar cell materials.

Importantly, as well known, the electro-negativity of oxygen atom is stronger than sulfur atom, so it is possible to reduce the HOMO level of the polymers by introducing furan moieties into polymers instead of thiophene ones. As a result, high open circuit voltage (V_{oc}) of the bulk heterojunction polymer solar cells can be expected, because the V_{oc} is related to the difference between the HOMO of the electron donor material and LUMO of the electron acceptor material.[12] In addition, furan derivatives can be synthesized from natural products; hence, the corresponding synthesis procedure can be realized by a simple, low-cost and sustainable method. Inspired by the purpose of giving deeper insight into the properties and functions of furans in conjugated polymers, it is necessity to further design and synthesis more furan-containing polymers for research.

Based on above mentioned issues, here we designed and synthesized a novel D-π-A copolymer, PFBT-BDT, as shown in Scheme 1a, with benzodithiophene (BDT) as the donor unit and bisoctyloxy substituted benzothiadiazole as the acceptor unit and furan as the bridged unit, to further explore new furan-containing polymers for the application as donor in PSCs. The polymer demonstrated good solubility in common organic solvents and a broad absorption in the wavelength range from 300 to 610 nm. The PSCs based on PFBT-BDT as the donor and [6,6] phenyl-C$_{71}$-butyric acid methyl ester (PC$_{71}$BM) as the acceptor exhibit a moderate PCE of 2.81% with a high V_{oc} of

[a]Key Laboratory of Carbon Fiber and Functional Polymers, Ministry of Education, College of Materials Science and Engineering, Beijing University of Chemical Technology, Beijing, 100029, China. E-mail: wanghaiqiao@mail.buct.edu.cn; lixy@mail.buct.edu.cn
[b]CAS Key Laboratory of Organic Solids, Institute of Chemistry, Chinese Academy of Sciences, Beijing, 100190, China. E-mail: liyf@iccas.ac.cn
[c]Division of Molecular and Materials Simulation, Key Lab for Nanomaterials, Ministry of Education, Beijing University of Chemical Technology, Beijing, 100029, China
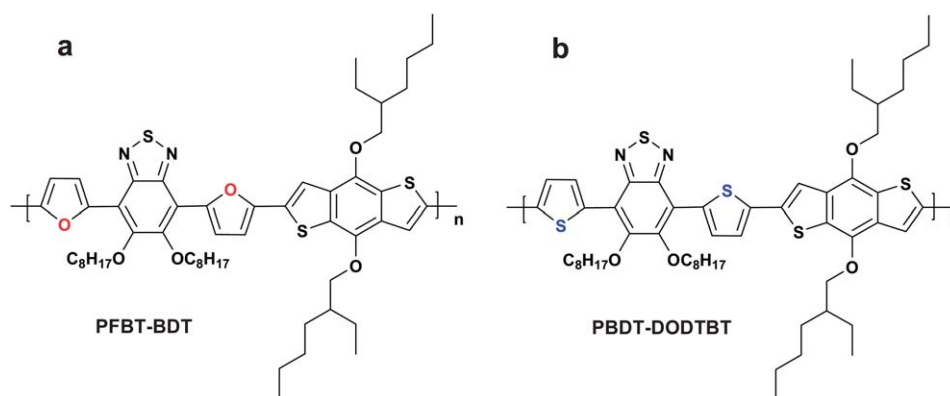
Scheme 1 Molecular structure of (a) **PFBT-BDT** and (b) **PBDT-DODTBT**.

0.94V under the illumination of AM 1.5G, 100 mW cm^{-2}. To the best of our knowledge, 0.94 V is among the highest V_{oc} values for PSCs based on benzodithiophene derivatives.

Experimental section

Materials

2,6-Bis(trimethyltin)-4,8-didodecyloxy-benzo[1,2-b;3,4-b]dithiophene (**BDP**),[1] and 4,7-dibromo-5,6-bis(octyloxy)benzo-2,1,3-thiadiazole (**1**)[13,14] were synthesized according to the literature. Tetrahydrofuran (THF) was dried over Na/benzophenone ketyl and freshly distilled prior to use. Other reagents and solvents were commercial grade and used as received without further purification. All reactions were performed under nitrogen atmosphere.

Measurements and characterization

The molecular weight of the polymer was measured using gel permeation chromatography (GPC). The GPC measurements were performed on a Waters 515–2410 with polystyrenes as the reference standard and tetrahydrofuran (THF) as an eluent. All new compounds were characterized by nuclear magnetic resonance spectra (NMR). The NMR was recorded on a Bruker AV 600 spectrometer at room temperature. Chemical shifts of ^{1}H NMR were reported in ppm. Splitting patterns were designated as s (singlet), t (triplet), d (doublet), m (multiplet), and br (broadened). Elemental analyses were performed on a Flash EA 1112 analyzer or Elementar vario EL III. Thermal gravimetric analysis (TGA, Netzsch TG209C) and the differential scanning calorimetry (DSC, TA-Q100) measurements were carried out under a nitrogen atmosphere at a heating rate of 10 °C min^{-1}. UV-Vis absorption spectra were recorded on a Shimadzu spectrometer model UV-3150. Absorption spectra measurements of the polymer solutions were carried out in chloroform (analytical reagent) at 25 °C. Absorption spectra measurements of the polymer films were carried out on the quartz plates with the polymer films spin-coated from the polymer solutions in chloroform (analytical reagent) at 25 °C. The electrochemical cyclic voltammetry was conducted on a Zahner IM6e electrochemical workstation with a Pt plate, Pt wire, and Ag/Ag$^+$ electrode as the working electrode, counter electrode, and reference electrode, respectively, in a 0.1 mol L^{-1} tetrabutylammonium

hexafluorophosphate (Bu$_4$NPF$_6$) acetonitrile solution. Polymer thin films were formed by drop-casting 1 mm^3 of polymer solutions in THF (analytical reagent, 1 mg mL^{-1}) on the working electrode and were then dried in air. Surface morphology of films was characterized on a Digital Instruments Multimode Nanoscope IIIa AFM by tapping mode in an ambient atmosphere.

Fabrication of photovoltaic devices

PSC was fabricated with ITO glass as a positive electrode, Ca/Al as a negative electrode, and the blend film of the polymer:PCBM between them as a photosensitive layer. The ITO glass was pre-cleaned and modified by a thin layer of PEDOT:PSS, which was spin-cast from a PEDOT:PSS aqueous solution (Clevious P VP AI 4083 H. C. Stark, Germany) on the ITO substrate, and the thickness of the PEDOT:PSS layer was about 60 nm. The photosensitive layer was prepared by spin-coating a blend solution of the polymer and PC$_{71}$BM with a weight ratio of 1 : 2 in o-dichlorobenzene on the ITO/PEDOT:PSS electrode. Then, the Ca/Al cathode was deposited on the polymer layer by vacuum evaporation under 3 × 10^{-4} Pa. The thickness of the photosensitive layer was ca. 80 nm, measured on an Ambios Tech XP-2 profilometer. The effective area of one cell was ca. 4 mm^2. The current–voltage (I versus V) measurement of the devices was conducted on a computer controlled Keithley 236 source measure unit. A xenon lamp with an AM 1.5 filter was used as the white-light source, and the optical power at the sample was 100 mW cm^{-2}.

Syntheses of the monomers

4,7-Difuran-2-yl-5,6-bis(octyloxy)benzo-2,1,3-thiadiazole (2). NaHCO$_3$ (5 g, 60 mmol) and 70 mL H$_2$O were added to a mixture of **1** (5.25 g, 15 mmol) and 2-furanboric acid (5 g, 45 mmol) in 200 mL THF was added . The solution was flushed with nitrogen for 10 min, and Pd(PPh$_3$)$_4$ (0.35 g, 0.3 mmol) was added. After another flushing with nitrogen for 20 min, the reactant was heated to reflux for 3 days. After cooling to room temperature, the reaction mixture was poured into saturated ammonium chloride solution. The product was extracted with ethyl acetate (3 × 100 ml). The extracts were combined and washed with water and brine then dried over anhydrous sodium sulfate. After filtration, the solvent was removed under reduced pressure. The

residue was purified by column chromatography on silica, eluting with petroleum ether/ethyl acetate (from 20 : 0 to 20 : 1), to give a yellow solid (6.2 g, 80%). ^{1}H NMR (600 MHz, CDCl$_3$): δ (ppm) 7.72 (d, 2H, Ar–H), 7.44 (d, 2H, Ar–H), 6.67 (dd, 2H, Ar–H), 4.12 (t, 4H, CH$_2$), 1.87 (m, 4H, CH$_2$), 1.48 (m, 4H, CH$_2$), 1.31–1.36 (m, 16H, CH$_2$), 0.92 (t, 6H, CH$_3$).

4,7-Bis(5-bromofuran-2-yl)-5,6-bis(octyloxy)benzo-2,1,3-thiadiazole (FBT). A mixture of **2** (2 g, 3.8 mmol), N-bromosuccimide (NBS) (1.4 g, 7.8 mmol), chloroform (50 mL) and acetic acid (50 mL) was stirred at room temperature in dark over night. Then the reaction mixture was poured into water (200 mL) and extracted with chloroform (3 × 50 ml). The extracts were combined and washed with water and saturated sodium bicarbonate solution then dried over anhydrous sodium sulfate. After filtration, the solvent was removed under reduced pressure. The residue was purified by column chromatography on silica, eluting with petroleum ether/chloroform (from 20 : 0 to 20 : 1), to give a bright yellow solid (1.77 g, 68%). ^{1}H NMR (600 MHz, CDCl$_3$): δ (ppm) 7.48 (d, 2H, Ar–H), 6.56 (d, 2H, Ar–H), 4.13 (t, 4H, CH$_2$), 1.93 (m, 4H, CH$_2$), 1.51 (m, 4H, CH$_2$), 1.25–1.38 (m, 16H, CH$_2$), 0.90 (t, 6H, CH$_3$). ^{13}C NMR (600 MHz, CDCl$_3$): δ (ppm) 152.64, 149.57, 149.52, 122.86, 116.51, 113.65, 113.44, 75.18, 31.85, 30.27, 29.58, 29.29, 26.12, 22.68, 14.10.

Synthesis of the polymer

FBT monomer (205 mg, 0.3 mmol) and **BDT** monomer (232 mg, 0.3 mmol) were put into a 25 mL two-neck flask, and 10 mL of toluene was added. The mixture was stirred and purged with nitrogen for 10 min, and then Pd(PPh$_3$)$_4$ (18 mg, 0.015 mmol) was added. After being purged for 15 min, the mixture was heated at 110 °C for 48 h. After cooled to room temperature, the reaction mixture was added dropwise to 200 mL acidic methanol, then collected by filtration and washed with methanol. The black solid was filtered into a Soxhlet funnel and extracted by methanol, hexane, and chloroform successively. The polymer recovered from chloroform was purified by preparative gel permeation chromatography. Then, the product was dried under vacuum for 1 day to recover the target polymer **PFBT-BDT** as a dark red solid. (yield 67.5%, M_n = 6.2kDa, M_w = 13.2kDa, PDI = 2.1). ^{1}H NMR (CDCl$_3$, 600 MHz): δ (ppm) 7.80 (br,2H), 7.61 (br, 2H), 6.96 (br, 2H), 4.25 (br, 8H), 1.99–1.22 (m, 52H), 1.11–0.82 (m, 18H). Anal. Calcd for (C$_{56}$H$_{74}$N$_2$O$_6$S$_2$)$_n$: C, 69.46; H, 7.65; N, 2.89. Found: C, 68.38; H, 7.65; N, 2.95.

Results and discussion

Syntheses of monomers and polymer

The synthesis routes of monomers and corresponding polymer are outlined in Schemes 2 and 3, respectively. First, compound **1** was prepared in five steps according to the procedure reported.[13,14] Then, two furan rings were attached to compound **1** by Suzuki coupling[15] using 2-furanboric acid as a reagent. Finally, compound **2** was brominated with NBS to give monomer **FBT** as a bright yellow solid in a 68% yield. The synthesis of the polymer was carried out using palladium-catalyzed Stille-coupling[16] between monomer **FBT** and **BDT**. All starting materials, reagents, and solvents were carefully purified, and all procedures

were performed under an air-free environment. The structure of the polymer was confirmed by ^{1}H NMR spectroscopy and elemental analysis. **PFBT-BDT** has good solubility in common organic solvents such as THF, chloroform and chlorobenzene. It can be readily processed to form smooth and pinhole-free films upon spin-coating.

Thermal analysis

The thermal properties of the polymer were determined by thermogravimetric analysis (TGA). **PFBT-BDT** has good thermal stability with onset decomposition temperature with 5% weight loss at 333 °C, as shown in Fig. 1, indicating that the thermal stability of the polymer is good enough for most applications.

Optical properties

Fig. 2 shows the absorption spectra of the polymer in chloroform solution and solid film on quartz plates. In chloroform solution, the polymer exhibited a broad absorption from 300 to 610 nm with three peaks at 343, 391 and 522 nm, respectively. In solid film, the absorption spectrum was expanded to 632 nm. Compared with its absorption in the solution, the absorption peaks of the polymer film were red shifted to 344, 398, and 534 nm, respectively, which is due to the aggregation of the molecular chains in the solid state. The optical band gap (E_g^{opt}) determined from the onset of absorption of **PFBT-BDT** film was 1.96 eV, which is a litter larger than that of the thiophene-based analogue **PBDT-DODTBT** (as shown in Scheme 1b) reported earlier by Ding et al.[17]

Electrochemical properties

Cyclic voltammetry has been employed and considered as an effective tool in determining the electronic energy levels of the conjugated oligomers and polymers.[18–21] From the onset oxidation and reduction potentials in the cyclic voltammogram, the highest occupied molecular orbital (HOMO) and lowest unoccupied molecular orbital (LUMO) energy levels can be readily estimated.

Cyclic voltammogram of the polymer film is shown in Fig. 3. The onset oxidation potential (E_{ox}) and onset reduction potential (E_{red}) of **PFBT-BDT** are 0.73 V vs. Ag/Ag$^+$ and −1.23 V vs. Ag/Ag$^+$, respectively. The HOMO and LUMO energy levels were calculated according the following equations:[18,19]

$$E_{HOMO} = -IP = -e(E_{ox} + 4.71) \text{ eV}$$

$$E_{LUMO} = -EA = -e(E_{red} + 4.71) \text{ eV}$$

Where the units of the onset redox potentials are V vs. Ag/Ag$^+$. The LUMO and HOMO energy levels of the polymer obtained are −3.48 eV and −5.44 eV, respectively. The electrochemical band gap of the polymer (E_g^{ec} = 1.96 eV) is matched very well with its optical band gap (E_g^{opt} = 1.96 eV). Compared to the HOMO level (−5.17 eV) of thiophene based analogue **PBDT-DODTBT**,[17] that of **PFBT-BDT** is about 0.27 eV lower, indicating that **PFBT-BDT** is more stable than **PBDT-DODTBT**.
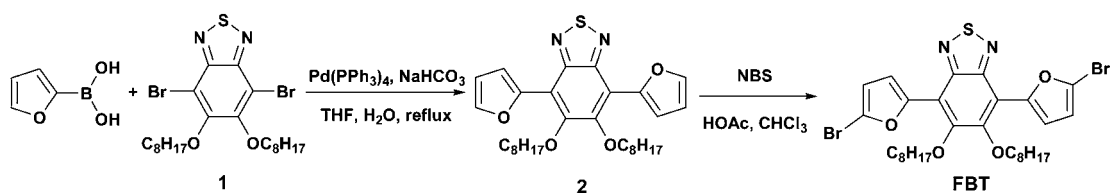
Scheme 2 Synthesis routes of the monomers.

This result also demonstrates that the replacement of thiophene moieties in conjugated polymers with furan ones is able to lower the HOMO energy levels, which means a higher V_{oc} could be expected, because V_{oc} is linearly correlated with the difference of the HOMO of the donor and the LUMO of the acceptor.[22,23]

Theoretical calculations

To provide further insight into the fundamentals of molecular architecture, density functional theory (DFT) calculations were performed to verify stationary points as stable states for the optimized conformations and single point energies, with a molecular main chain length $n = 1$, at B3LYP/6-31 + g(3df,3pd) level using the Gaussian 03 program package. The final energies were calculated as the sum of single point and zero point energies. Moreover, all the C_nH_{2n+1}– side chains were replaced with CH_3– in the calculation to avoid excessive computation demand, since they do not significantly affect the electronic properties.

Ionization potential (IP) and electron affinity (EA) calculated were -5.2149 eV and -2.7858 eV, with the corresponding band gap of 2.4291 eV. The wave functions of the frontier molecular orbitals are depicted in Fig. 4. As can be observed, the HOMO is delocalized along the whole π-conjugated backbone while the LUMO is mostly concentrated on the benzothiadiazole-based acceptor groups. These images provide further evidence of the formation of well-defined D-π-A structure and the intramolecular charge transfer (ICT) behavior of the material (*i.e.*, the HOMO to LUMO transition is a donor to acceptor intramolecular charge transfer).[24]

Morphology of the blend film of PFBT-BDT and PC$_{71}$BM

The morphology feature of the photoactive layer is very important for the performance of PSCs.[25] Here, atomic force microscopy (AFM) was used to characterize the surface morphology of
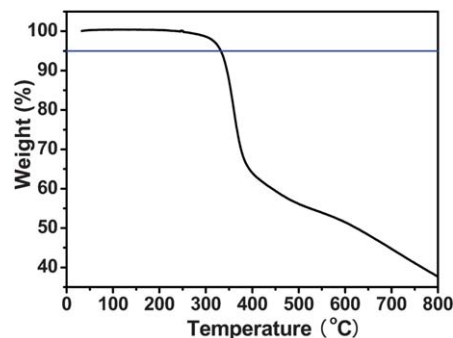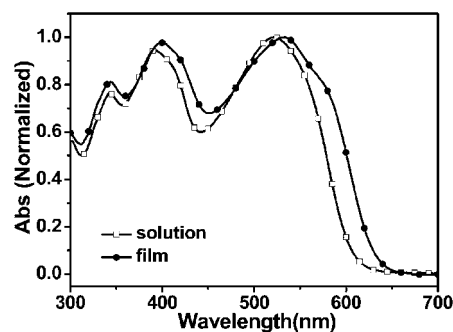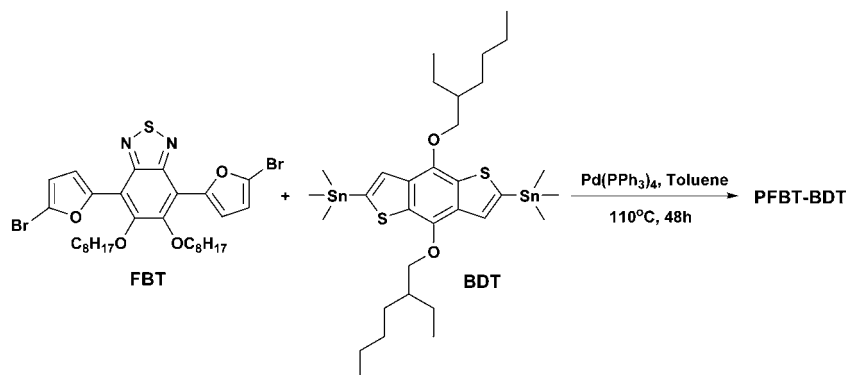

Fig. 1 TGA plot of the polymer with a heating rate of 10 °C min^{-1} under an inert atmosphere.

Fig. 2 Normalized absorption spectra of **PFBT-BDT** in chloroform solution and solid film on quartz plates.

active layers of PSCs. As shown in Fig. 5, the topography of the film obtained from **PFBT-BDT**: PC$_{71}$BM (1 : 2) in dichlorobenzene is smooth (RMS = 1.1 nm, R_a = 0.32 nm). The polymer and fullerene domains are uniformly distributed throughout the
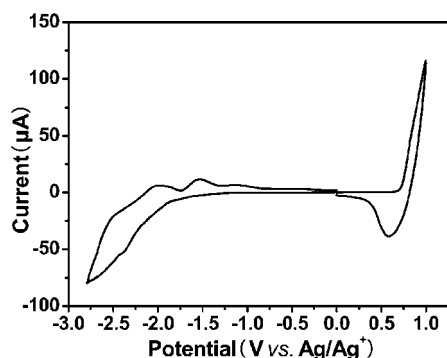
Scheme 3 Synthetic route of the copolymer.

Fig. 3 Cyclic voltammogram of the polymer film on Pt electrode in 0.1 mol L^{-1} Bu$_4$NPF$_6$, CH$_3$CN solution with a scan rate of 100 mV s^{-1}.

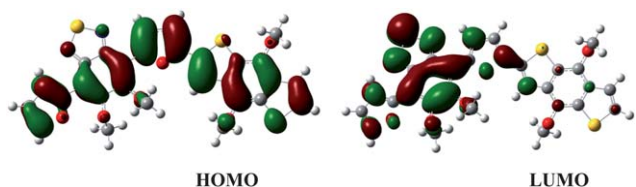**HOMO**   **LUMO**

Fig. 4 B3LYP/6-31g(3df,3pd) wave functions of the frontier molecular orbital (HOMO, left; LUMO, right) in **PFBT-BDT** with a chain length $n = 1$.

surface of the film, in other words, the nanometre-scale interpenetrating network has be formed in this blend, which can benefit not only the charge separation but also the charge transport.

Photovoltaic properties of the polymer

In this paper, the motivation of the design and synthesis of the polymer is to look for a novel alternating copolymer based on furan substituted benzothiadiazole derivative for the application in solar cells. So, we fabricated the device with the structure of ITO/PEDOT: PSS/polymer:PC$_{71}$BM (1 : 2 w/w)/Ca/Al, where the polymer was used as the electron donor and PC$_{71}$BM was used as the electron acceptor, and the performance of the PSC was investigated tentatively. Fig. 6 shows the J–V curve of the PSC under the illumination of AM 1.5, 100 mW cm^{-2}. It showed

a PCE of 2.81% with an open circuit voltage (V_{oc}) of 0.94 V, a short circuit current density (J_{sc}) of 6.5 mA cm^{-2}, and a fill factor (FF) of 0.46, without annealing and any additives. The PSC demonstrated a moderate PCE and J_{sc} and high V_{oc} value. The V_{oc} value is about 0.2 V higher than that of the device based on thiophene-based analogue **PBDT-DODTBT**.[17] To the best of our knowledge, 0.94 V is among the highest V_{oc} values for PSCs based on benzodithiophene derivatives. The high value of V_{oc} of the device based on **PFBT-BDT** benefits from the low HOMO energy level of the polymer. The external quantum efficiency (EQE) spectrum of the device is shown in Fig. 7. The device exhibited photoresponse spectrum covering from 300 to 650 nm with an EQE value of more than 30% in the region between 360 and 560 nm. The integration of the EQE values agrees well with the J_{sc} of 6.5 mA cm^{-2}. It is worth noting that the PSCs fabricated from a blend of furan-containing polymers, **PDPP2FT** and **PDPP3F**, reported earlier by Woo *et al.*,[11] with PC$_{71}$BM demonstrated poor PCE (<1%), but the PCE can be greatly improved to 5% with the addition of additive 1-chloronaphthalene (CN). If PC$_{61}$BM was used as an alternative to PC$_{71}$BM, PSC devices afforded more than 3.0% PCE (max. 3.8%), whereas the use of CN led to a slight improvement of PCE. In an attempt to improve the PCE of PSCs based on **PFBT-BDT**, we also used the additive CN to optimize blend morphology. Unfortunately, the device performance cannot be improved. This result manifests that other additives and different device conditions must be
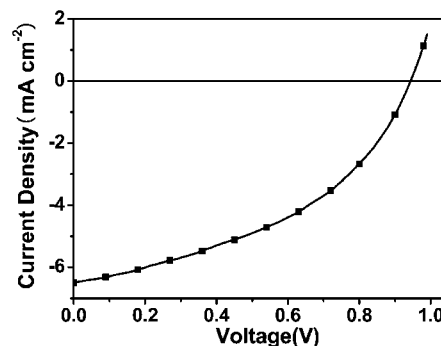

Fig. 6 Current density-voltage characteristic of the PSC based on **PFBT-BDT**:PC$_{71}$BM (1 : 2, w/w), under the illumination of AM1.5G, 100 mW cm^{-2}.
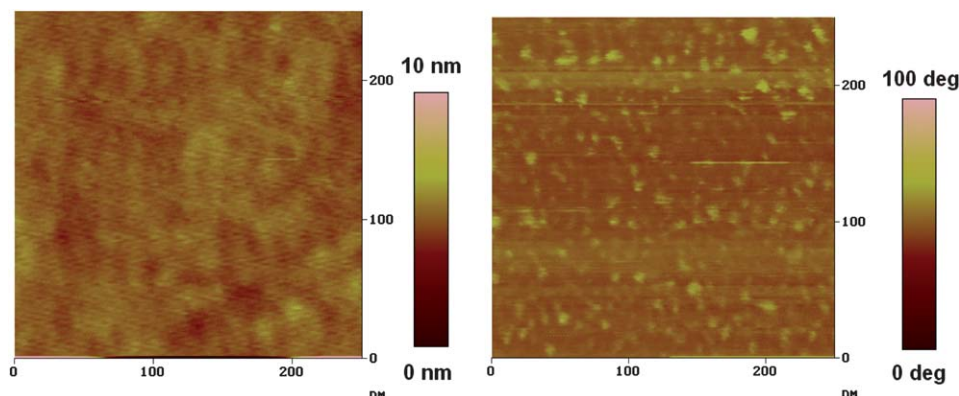

Fig. 5 Tapping mode AFM topography (left) and phase (right) images of **PFBT-BDT**: PC$_{71}$BM (1 : 2) film.
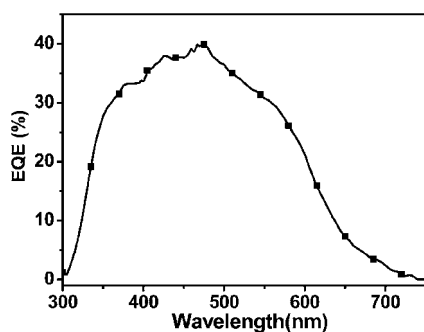
Fig. 7 The external quantum efficiency (EQE) spectrum of the PSC based on **PFBT-BDT**:PC$_{71}$BM (1 : 2, w/w).

tried for further improving the device performance. This work is still ongoing and a higher PCE is anticipated. Even so, the current device performance, which is 3 times higher than the PCE of devices based on **PDPP2FT** and **PDPP3F** with the same device configuration without CN additive, indicates that **PFBT-BDT** would be a promising photovoltaic material.

Conclusion

We designed and synthesized a novel furan-containing benzo-thiadiazole derivative based D-π-A polymer (**PFBT-BDT**). The polymer demonstrated good thermal stability (T_d > 330 °C), good solubility in common organic solvents, and a deep HOMO energy level at −5.44 eV. The polymer solar cell fabricated from the blend of **PFBT-BDT**:PC$_{71}$BM exhibited moderate PCE of 2.81% with a high V_{oc} of 0.94 V, which benefits from the deep HOMO level of the polymer. Further improvements on device performance through device engineering as well as a structure optimization of polymer are in progress. These results demonstrate the potential of the replacement of thiophene with furan units in the design and synthesis of conjugated polymers with efficient solar cell performance, and especially to lower the HOMO energy levels of the conjugated polymers, therefore, increase the open circuit voltage of solar cells. Most importantly, this work opens up a new path to design high performance photovoltaic materials.

Acknowledgements

References

1 J. H. Hou, H. Y. Chen, S. Q. Zhang, R. I. Chen, Y. Yang, Y. Wu and G. Li, *J. Am. Chem. Soc.*, 2009, **131**, 15586.
2 H. Y. Chen, J. H. Hou, S. Q. Zhang, Y. Y. Liang, G. W. Yang, Y. Yang, L. P. Yu, Y. Wu and G. Li, *Nat. Photonics*, 2009, **3**, 649.
3 M. Wang, X. W. Hu, P. Liu, W. Li, X. Gong, F. Huang and Y. Cao, *J. Am. Chem. Soc.*, 2011, **133**, 9638.
4 L. J. Huo, X. Guo, S. Q. Zhang, Y. F. Li and J. H. Hou, *Macromolecules*, 2011, **44**, 4035.
5 H. Bronstein, Z. Y. Chen, R. S. Ashraf, W. M. Zhang, J. P. Du, J. R. Durrant, P. S. Tuladhar, K. Song, S. E. Watkins, Y. Geerts, M. M. Wienk, R. A. J. Janssen, T. Anthopoulos, H. Sirringhaus, M. Heeney and I. McCulloch, *J. Am. Chem. Soc.*, 2011, **133**, 3272.
6 Y. Huang, L. J. Huo, S. Q. Zhang, X. Guo, C. C. Han, Y. F. Li and J. H. Hou, *Chem. Commun.*, 2011, **47**, 8904.
7 T. Y. Chu, J. P. Lu, S. Beaupr, Y. G. Zhang, J. R. Pouliot, S. Wakim, J. Y. Zhou, M. Leclerc, Z. Li, J. F. Ding and Y. Tao, *J. Am. Chem. Soc.*, 2011, **133**, 4250.
8 S. C. Price, A. C. Stuart, L. Q. Yang, H. X. Zhou and W. You, *J. Am. Chem. Soc.*, 2011, **133**, 4625.
9 H. X. Zhou, L. Q. Yang, A. C. Stuart, S. C. Price, S. B. Liu and W. You, *Angew. Chem., Int. Ed.*, 2011, **50**, 2995.
10 B. Walker, A. B. Tomayo, X. D. Dang, P. Zalar, J. H. Seo, A. Garcia, M. Tantiwiwat and T. Q. Nguyen, *Adv. Funct. Mater.*, 2009, **19**, 3063.
11 C. H. Woo, P. M. Beaujuge, T. W. Holcombe, O. P. Lee and J. M. J. Frechet, *J. Am. Chem. Soc.*, 2010, **132**, 15547.
12 M. C. Scharber, D. Muhlbacher, M. Koppe, P. Denk, C. Waldauf, A. J. Heeger and C. J. Brabec, *Adv. Mater.*, 2006, **18**, 789.
13 R. P. Qin, W. W. Li, C. H. Li, C. Du, C. Veit, H. F. Schleiermacher, M. Andersson, Z. S. Bo, Z. P. Liu, O. Inganas, U. Wuerfel and F. L. Zhang, *J. Am. Chem. Soc.*, 2009, **131**, 14612.
14 F. Y. Qing, Y. P. Sun, X. C. Wang, N. Li, Y. F. Li, X. Y. Li and H. Q. Wang, *Polym. Chem.*, 2011, **2**, 2102.
15 X. C. Wang, H. Q. Wang, Y. Yang, Y. J. He, L. Zhang, Y. F. Li and X. Y. Li, *Macromolecules*, 2010, **43**, 709.
16 Z. N. Bao, W. K. Chan and L. P. Yu, *J.Am. Chem. Soc.*, 1995, **117**, 12426.
17 P. Ding, C. C. Chu, B. Liu, B. Peng, Y. P. Zou, Y. H. He, K. C. Zhou and C. S. Hsu, *Macromol. Chem. Phys.*, 2010, **211**, 2555.
18 Y. F. Li, Y. Cao, J. Gao, D. L. Wang, G. Yu and A. J. Heeger, *Synth. Met.*, 1999, **99**, 243–248.
19 Q. J. Sun, H. Q. Wang, C. H. Yang and Y. F. Li, *J. Mater. Chem.*, 2003, **13**, 800.
20 J. H. Hou, Z. A. Tan, Y. Yan, Y. J. He, C. H. Yang and Y. F. Li, *J. Am. Chem. Soc.*, 2006, **128**, 4911.
21 C. L. Lu, H. Q. Wang, X. C. Wang, Y. F. Li, T. Oiu, L. F. He and X. Y. Li, *J. Appl. Polym. Sci.*, 2010, **117**, 517.
22 M. C. Scharber, D. M. hlbacher, M. Koppe, P. Denk, C. Waldauf, A. J. Heeger and C. J. Brabec, *Adv. Mater.*, 2006, **18**, 789.
23 L. J. Huo, J. H. Hou, S. Q. Zhang, H. Y. Chen and Y. Yang, *Angew. Chem., Int. Ed.*, 2010, **122**, 1542.
24 T. M. Pappenfus, D. K. Schneiderman, J. Casado, J. T. L. Navarrete, M. C. R. Delgado, G. Zotti, B. Vercelli, M. D. Lovander, L. M. Hinkle, J. N. Bohnsack and K. R. Mann, *Chem. Mater.*, 2011, **23**, 823.
25 C. V. Hoven, X. D. Dang, R. C. Coffin, J. Peet, T. Q. Nguyen and G. C. Bazan, *Adv. Mater.*, 2010, **22**, E63.